Whisker Embedding Impedance for Millimeter Wave Diode Circuits

Jie Xu and Antti V. Räisänen

Radio Laboratory, Helsinki University of Technology
Otakaari 5A, SF-02150 Espoo, Finland

Abstract

This paper reports our newer developments on theoretical modeling of a whisker mounted in a rectangular waveguide. The moment method in conjunction with the dyadic Green's function is employed to analyze this structure. Effects of whiskers with various types of shape on the embedding impedance are investigated and presented.

I. Introduction

A metal whisker mounted in a rectangular waveguide filled with an isotropic and homogeneous medium (μ, ϵ), as shown in Fig. 1, has found extensive applications in constructing millimeter wave circuits. Though some experimental studies on the structure have been done, see for example [1,2], only until recently some efforts have been carried out on the theoretical modeling work in [3]. This paper reports our further development on theoretical impedance modeling of the whisker mount whose arc part is approximated by some pieces of slant wires as shown in Fig. 1. Hereby we refer to as the first-order modeling to the whisker geometry in comparison with the zeroth-order modeling in [3], in which the arcs of the whisker is approximated by a cascade of some horizontal and vertical pieces of straight wires, as also shown in Fig.1. The moment method in conjunction with the dyadic Green's function in a rectangular waveguide is employed to analyze the whisker structure. The waveguide walls and the whisker are assumed to be perfect conductors and main attention is given to the electrical property of the small whisker. The analytical results show good agreement with experimental results and can be expected to provide fundamental guidance for the circuit design utilizing a whisker mount. Effects of whiskers with various types of shape on the embedding impedance are investigated. Results for whiskers located in a cross-sectional plane of a rectangular waveguide are presented. Effects of whisker orientations on its radiating property will appear in a coming paper.

II. Theory

A. First-Order Modeling

Referring to the whisker configuration shown in Fig. 1 and applying a voltage V across the infinitesimal excitation gap, the excited current $\mathbf{J}(\mathbf{r})$ along the whisker surface may be expressed as

$$\mathbf{J}(\mathbf{r}) = \sum_{l=1}^{L} J_l \mathbf{B}_l(\mathbf{r}), \tag{1}$$

where J_l is the current expansion coefficient, $\mathbf{B}_l(\mathbf{r})$ is the current expansion basis function. Since the angular variation of the surface current makes little contribution to the embedding impedance of a whisker with an electrically small diameter [3,4], the current distribution is approximated by a group of surface current multifilaments parallel to the whisker axis. And each filament is modeled by a cascade of straight lines. The L in (1) is the total segmentation number.

In the case that the whisker is located in a transversal plane of a rectangular waveguide, the current expansion coefficient J_l can be determined by application of the moment method with the Galerkin's technique [3] from the following linear matrix equation

$$[Z_l^q][J_l] = [V_q], \quad q, l = 1, ..., L \tag{2}$$

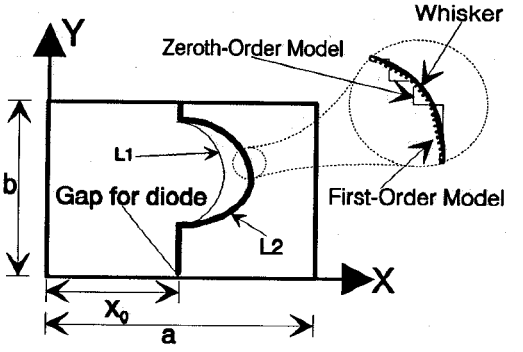

Fig. 1 Schematic drawing of waveguide whisker mounts placed in a Cartesian coordinates, and two models for whisker geometry. $X_0 = a/2$. L_1 and L_2 are the two whiskers to be modeled.

OF1

CH3277-1/93/0000-0333$01.00 © 1993 IEEE

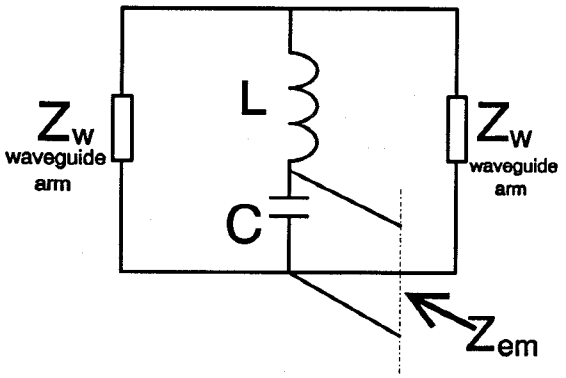

Fig. 2 Equivalent circuit for a whisker mount which is located in a cross-sectional plane of a rectangular waveguide. Only the TE_{10} mode is assumed to propagate in the waveguide.

where

$$V_q = \int_{\Delta S_q} W_q(r) E^{im}(r) dl, \tag{3}$$

and $E^{im}(r)$ is the electric field impressed on the excitation gap, $W_q(r)$ is the weighting function, ΔS_q is the q-th segment,

$$Z_{ql} = S_{xx} + S_{xy} + S_{yx} + S_{yy}, \tag{4}$$

where

$$S_{xx} = \frac{\Delta x}{|\Delta x|}\frac{\Delta x'}{|\Delta x'|}\frac{j\eta}{2abk}\sum_{m=0}^{\infty}\epsilon_{0m}[k^2 - k_x^2]\cdot$$

$$\{\sum_{n=1}^{\infty}\epsilon_{0n}\left(\frac{e^{-\Gamma_{mn}|z_d|}}{\Gamma_{mn}} - \frac{e^{-\gamma_{mn}|z_d|}}{\gamma_{mn}}\right) I_{xx1} + \frac{b}{\pi}\sum_{n=-\infty}^{\infty} I_{xx2}\}, \tag{5}$$

$$S_{yy} = jk\eta\{\sum_{n=1}^{\infty}\frac{(k^2 - k_y^2)}{\pi bk^2}\sum_{m=-\infty}^{\infty}\frac{\Delta y}{|\Delta y|}\frac{\Delta y'}{|\Delta y'|} I_{yy1}$$

$$+ \sum_{m=1}^{\infty}\left(\frac{e^{-\Gamma_{m0}|z_d|}}{ab\Gamma_{m0}} - \frac{e^{-k_x|z_d|}}{abk_x}\right) I_{yy2} + \frac{1}{4\pi b}\frac{\Delta y}{|\Delta y|}\frac{\Delta y'}{|\Delta y'|} I_{yy3}\}, \tag{6}$$

$$S_{xy} = jk\eta\sum_{n=1}^{\infty}\sum_{m=-\infty}^{\infty}\frac{(-k_y k_n)}{\pi bk^2}\frac{\Delta x}{|\Delta x|}\frac{\Delta y'}{|\Delta y'|}\int_{\Delta x}\int_{\Delta y'}\sin k_y y\cdot$$

$$\cos k_y y'\{\frac{x_+}{U_+}K_1[k_n U_+] - \frac{x_-}{U_-}K_1[k_n U_-]\}dxdy', \tag{7}$$

$$S_{yx} = jk\eta\sum_{n=1}^{\infty}\sum_{m=-\infty}^{\infty}\frac{(-k_y k_n)}{\pi bk^2}\frac{\Delta y}{|\Delta y|}\frac{\Delta x'}{|\Delta x'|}\int_{\Delta y}\int_{\Delta x'}\cos k_y y\cdot$$

$$\sin k_y y'\{\frac{x_+}{U_+}K_1[k_n U_+] + \frac{x_-}{U_-}K_1[k_n U_-]\}dydx'. \tag{8}$$

where

$$I_{xx1} = \int_{\Delta x}\int_{\Delta x'} F_{xx}(x,x')\sin(k_y y)\sin(k_y y')dx'dx, \tag{9}$$

$$I_{xx2} = \int_{\Delta x}\int_{\Delta x'} F_{xx}(x,x')\{K_0[k_m V_-] - K_0[k_m V_+]\}dx'dx, \tag{10}$$

$$I_{yy1} = \int_{\Delta y}\int_{\Delta y'} F_{yy}(y,y')\{K_0[k_n U_-] - K_0[k_n U_+]\}dydy', \tag{11}$$

$$I_{yy2} = \frac{\Delta y}{|\Delta y|}\frac{\Delta y'}{|\Delta y'|}\int_{\Delta y}\int_{\Delta y'}\sin k_x x \sin k_x x' dydy', \tag{12}$$

$$I_{yy3} = \int_{\Delta y}\int_{\Delta y'}\ln\frac{\cosh\frac{\pi|z_d|}{a} - \cos\frac{\pi}{a}(x+x')}{\cosh\frac{\pi|z_d|}{a} - \cos\frac{\pi}{a}(x-x')}dydy', \tag{13}$$

$$F_{xx}(x,x') = \cos(k_x x)\cos(k_x x') \tag{14}$$

$$F_{yy}(y,y') = \cos(k_y y)\cos(k_y y'), \tag{15}$$

with

$$V_\pm = \sqrt{|z_d|^2 + (2nb + y_\pm)^2}, y_\pm = y \pm y', z_d = z - z',$$

$$U_\pm = \sqrt{|z_d|^2 + x_\pm^2}, x_\pm = 2ma + x \pm x',\ k_n = \sqrt{k_y^2 - k^2},$$

$$\gamma_{mn} = \sqrt{k_c^2 + k^2},\ k_m = \sqrt{k_x^2 + k^2},\ k = \omega\sqrt{\mu_0\epsilon_0}. \tag{16}$$

where ω is the angular operating frequency.

Upon determination of the current distribution on the whisker, the embedding impedance Z_{em} looking at the excitation point may be readily evaluated as

$$Z_{em} = -\frac{\int_{whisker} E\cdot J dl}{I^2(0)}. \tag{17}$$

In case that the whisker is located on a cross-sectional plane of the waveguide, the structure can be described by the equivalent circuit shown in Fig. 2. The capacitance **C** and the inductance **L** can be directly de-embedded from Z_{em} as in [3].

B. Numerical Calculations

Special care has to be taken when calculating the generalized impedance matrix components. Except the intrinsic singularity of the dyadic Green's function of rectangular waveguides should be addressed properly, both the double infinite series and the integrals contained in each matrix component have to be computed accurately and efficiently. A multifilament model can be used to circumvent the first obstacle, in which case the current distribution is approximated by current multifilaments and the observation

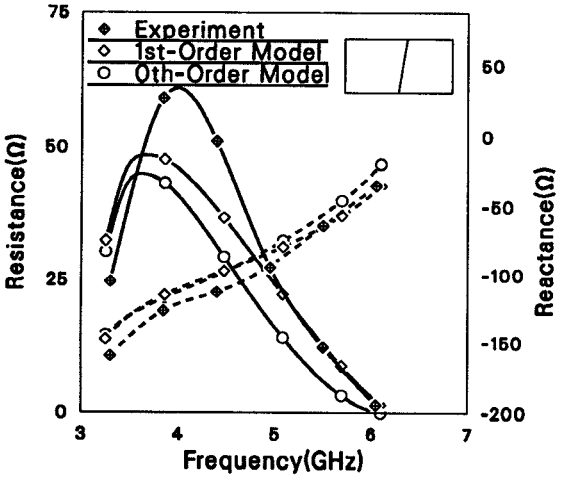

Fig. 3 Comparisons of embedding impedance (Z_{em} in Fig.2) from the zeroth-order and first-order modeling with experimental results for a slant post with a 10° tilt angle with respect to the waveguide narrow side (Y axis in Fig. 1). Post diameter 3 *mm*. Waveguide a=47.6 *mm*, b=22.15 *mm*. —— for resistance, – – – for reactance.

points are only chosen to be between the current filaments. This technique has been proven to be efficient and successful [3,4].

The double infinite series in the dyadic Green's functions converges extremely slow and can not directly be used in the numerical applications [5,6]. The Poisson summation formula can be used to convert one sum of the double infinite summation into a Fourier domain summation and thus accelerates convergence. The other sum may be handled with partial summation technique [6] or some series acceleration procedures [7]. The partial summation technique has been applied in present work.

The integrals in (7)~(13) can be evaluated explicitly when whisker segments are parallel to either of the waveguide walls, i.e., a and b, and then the summations are easier to be handled [3]. The evaluations of the numerical integrals will greatly increase the whole computation time when dealing with whisker segments with some tilt angles. The integrals above are numerically evaluated.

III. Results

Based on the computer code used in [3], another program has been written to implement the first-order modeling of the whisker structure. The pulse function has been chosen as both the basis function and weighting function. The singular value decomposition method is utilized to solve the matrix equation (2) after the generalized impedance matrix components are determined.

A lot of structures including whiskers shown in Fig. 1 have been modeled in terms of this formulation. The inset plots in the upper right corner of each figure to be presented below depict the whisker geometry for modeling.

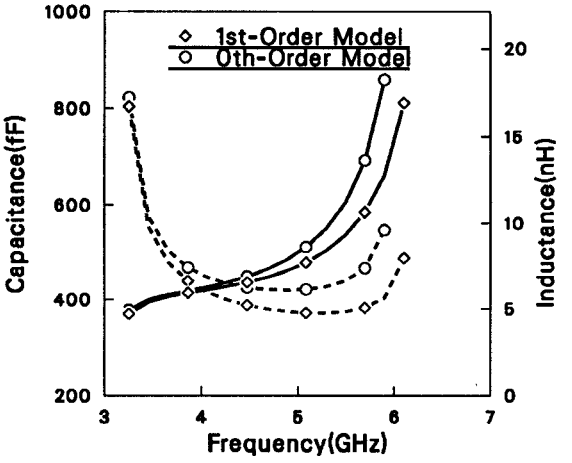

Fig. 4 Comparisons of the equivalent circuit parameters derived from the zeroth-order and first-order modelings for the slant post shown in Fig.3. —— for capacitance, – – – for inductance.

The validity of the formulation is first checked by modeling a slant post with a 10° tilt angle with respect to the waveguide narrow side. A fair well agreement between present calculations and the experimental results can be found in Fig. 3 and Fig. 4. For the convenience of comparison, the embedding impedance derived from the zeroth-order modeling [3] is also depicted in these figures. It can be seen that a solution better in agreement with the experiment has been obtained with the first-order modeling than with the zeroth-order modeling. It can easily be understood because the first-order modeling uses a better approximation to the whisker geometry.

Another two whiskers which consist of a cascade of linear segments with some tilt angles to either of the waveguide walls have also been modeled. The operating frequency is chosen to be in 100~250 GHz range. The embedding impedances for these two whiskers are plotted in Fig. 5 and Fig. 6. And the frequency dependences of the lumped-circuit equivalent parameters of these two whiskers are compared in Fig. 7.

IV. Remarks

A further effort has been carried out to theoretically model the rectangular waveguide whisker mount which finds extensive applications in millimeter wave circuit constructions. The whole modeling work is based on the moment method in conjunction with successful applications of the dyadic Green's function for rectangular waveguides. One can see from the preceding computations that the whisker shape would greatly affect its embedding impedance presented to the active device, and secondly a constant inductance or capacitance assumption for a whisker mount in a rectangular waveguide may contribute large discrepencies to circuit performance compared with theoretical designs because of the strong dependance of the lumped circuit parameters on operating frequency.

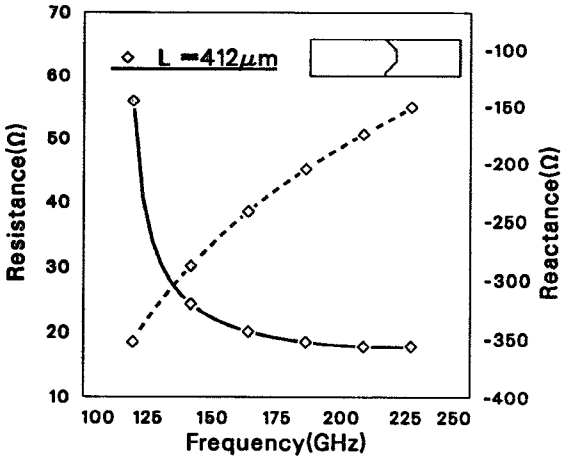

Fig. 5 Embedding impedance (Z_{em} in Fig.2) for a whisker that constitutes a cascade of linear segments with some tilt angles to waveguide walls. Whisker length $L_1 = 0.412\ mm$, diameter 12.7 μm. Waveguide a=1.3 mm, b=0.33 mm. —— for resistance, – – – for reactance.

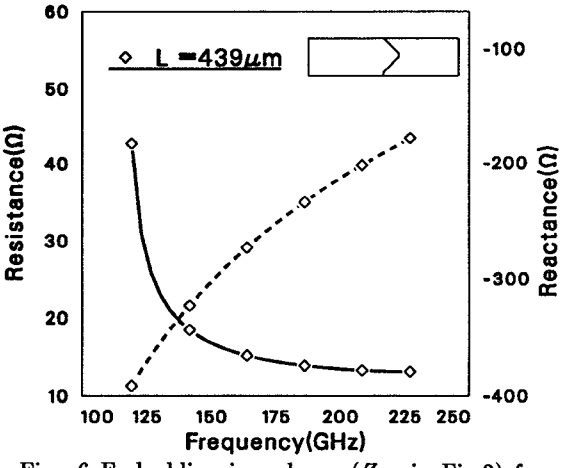

Fig. 6 Embedding impedance (Z_{em} in Fig.2) for a whisker that constitutes a cascade of linear segments with some tilt angles to waveguide walls. Whisker length $L_2 = 0.439\ mm$, diameter 12.7 μm. Waveguide a=1.3 mm, b=0.33 mm. —— for resistance, – – – for reactance.

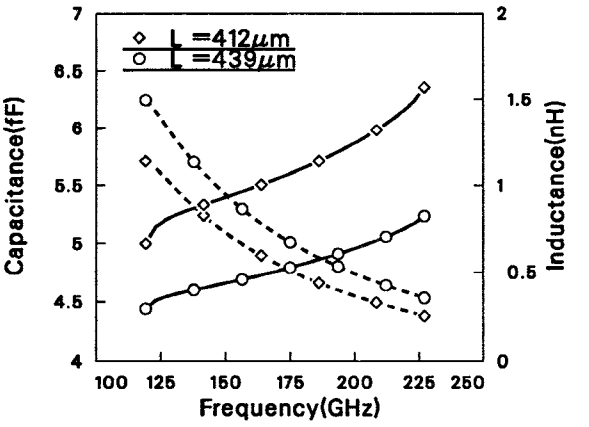

Fig. 7 Frequency dependence of the equivalent circuit parameters of the whiskers shown in Fig.5 and Fig.6. —— for capacitance, – – – for inductance.

REFERENCES

[1] C.E. Hagström and E.L. Kollberg, "Measurements of embedding impedance of millimeter wave diode mounts," *IEEE Trans. Microwave Theory Tech.*, Vol. MTT-28, pp. 899-904, August 1980.

[2] A.O. Lehto and A.V. Räisänen, "Embedding impedance of a millimeter wave Schottky mixer: scaled model measurements and computer simulations," *Int. J. Infrared Millimeter Waves*, pp. 609-628, Vol. 4, No. 4, 1983.

[3] J. Xu and A.V. Räisänen, "Impedance modeling of a whisker mounted in a rectangular waveguide," to appear in *IEEE Microwave Guided Wave Letters*, Vol. 3, No. 3, 1993.

[4] J.M. Jarem, "A multifilament method-of-moments solution for the input impedance of a probe-excited semi-infinite waveguide" *IEEE Trans. Microwave Theory Tech.*, Vol. MTT-35, pp. 14-19, Jan. 1987.

[5] Y. Rahmat-Samii, "On the question of computations of the dyadic Green's function at the source region in waveguides and cavities," *IEEE Trans. Microwave Theory Tech.*, Vol. MTT-23, pp. 762-765, Sept. 1975.

[6] J.J.H. Wang, "Analysis of a three-dimensional arbitrarily shaped dielectric or biological body inside a rectangular waveguide," *IEEE Trans. Microwave Theory Tech.*, Vol. MTT-26, pp. 457-462, July 1978.

[7] S. Singh and R. Singh, "Application of transforms to accelerate the summation of periodic free-space Green's functions," *IEEE Trans. Microwave Theory Tech.*, Vol. MTT-38, pp. 1746-1748, Nov. 1990.

[8] R.L. Eisenhart and P.J. Khan, " Theoretical and experimental analysis of a waveguide mounting structure, " *IEEE Trans. Microwave Theory Tech.*, Vol. MTT-19, pp. 706-719, Aug. 1971.